

UC Berkeley

UC Berkeley Previously Published Works

Title

Hippocampal Connectivity with Retrosplenial Cortex is Linked to Neocortical Tau Accumulation and Memory Function.

Permalink

<https://escholarship.org/uc/item/6mg5t2sj>

Journal

Journal of Neuroscience, 41(42)

ISSN

0270-6474

Authors

Ziontz, Jacob
Adams, Jenna N
Harrison, Theresa M
et al.

Publication Date

2021-10-20

DOI

10.1523/jneurosci.0990-21.2021

Peer reviewed

Hippocampal Connectivity with Retrosplenial Cortex is Linked to Neocortical Tau Accumulation and Memory Function

 Jacob Ziontz,¹  Jenna N. Adams,¹ Theresa M. Harrison,¹  Suzanne L. Baker,² and  William J. Jagust^{1,2}

¹Helen Wills Neuroscience Institute, UC Berkeley, Berkeley, California 94720, and ²Molecular Biophysics and Integrated Bioimaging, Lawrence Berkeley National Laboratory, Berkeley, California 94720

The mechanisms underlying accumulation of Alzheimer's disease (AD)-related tau pathology outside of the medial temporal lobe (MTL) in older adults are unknown but crucial to understanding cognitive decline. A growing body of evidence from human and animal studies strongly implicates neural connectivity in the propagation of tau in humans, but the pathways of neocortical tau spread and its consequences for cognitive function are not well understood. Using resting state functional magnetic resonance imaging (fMRI) and tau PET imaging from a sample of 97 male and female cognitively normal older adults, we examined MTL structures involved in medial parietal tau accumulation and associations with memory function. Functional connectivity between hippocampus (HC) and retrosplenial cortex (RsC), a key region of the medial parietal lobe, was associated with tau in medial parietal lobe. By contrast, connectivity between entorhinal cortex (EC) and RsC did not correlate with medial parietal lobe tau. Further, greater hippocampal-retrosplenial (HC-RsC) connectivity was associated with a stronger correlation between MTL and medial parietal lobe tau. Finally, an interaction between connectivity strength and medial parietal tau was associated with episodic memory performance, particularly in the visuospatial domain. This pattern of tau accumulation thus appears to reflect pathways of neural connectivity, and propagation of tau from EC to medial parietal lobe via the HC may represent a critical process in the evolution of cognitive dysfunction in aging and AD.

Key words: episodic memory; functional connectivity; hippocampus; medial parietal; retrosplenial; tau

Significance Statement

The accumulation of tau pathology in the neocortex is a fundamental process underlying Alzheimer's disease (AD). Here, we use functional connectivity in cognitively normal older adults to track the accumulation of tau in the medial parietal lobe, a key region for memory processing that is affected early in the progression of AD. We show that the strength of connectivity between the hippocampus (HC) and retrosplenial cortex (RsC) is related to medial parietal tau burden, and that these tau and connectivity measures interact to associate with episodic memory performance. These findings establish the HC as the origin of medial parietal tau and implicate tau pathology in this region as a crucial marker of the beginnings of AD.

Introduction

Hyperphosphorylation of the microtubule-associated protein tau together with amyloid- β ($A\beta$) plaques represent the hallmark neuropathologies of Alzheimer's disease (AD). Early histopathology studies (Braak and Braak, 1991) and more recent positron emission tomography (PET) imaging have characterized the distribution and extent of pathologic tau burden in patients with AD as well as cognitively healthy older adults (Johnson et al., 2016; Schöll et al., 2016). Tau pathology has been observed to originate in the transentorhinal region, an area spanning the lateral entorhinal cortex (EC) and medial perirhinal cortex in humans (Braak and Braak, 1985, 1995), but its accumulation in cortical areas outside of the medial temporal lobe (MTL), perhaps facilitated by $A\beta$ (He et al., 2018), is often a feature of the earliest stages of AD.

Received May 10, 2021; revised Aug. 27, 2021; accepted Aug. 30, 2021.

Author contributions: J.Z., J.N.A., T.M.H., and W.J.J. designed research; J.Z. and S.L.B. performed research; J.Z. analyzed data; J.Z. wrote the first draft of the paper; J.Z., J.N.A., T.M.H., S.L.B., and W.J.J. edited the paper; J.Z. and W.J.J. wrote the paper.

This work was supported by National Institutes of Health Grants T32-NS095939 (to J.Z.), F31-AG062090 (to J.N.A.), F32-AG057107 (to T.M.H.), R01-AG062542 (to W.J.J.), and R01-AG034570 (to W.J.J.) and by the Rainwater Charitable Foundation (W.J.J.). Avid Radiopharmaceuticals enabled the use and the ¹⁸F-Flortaucipir tracer but did not provide direct funding and were not involved in data analysis or interpretation. We thank R. La Joie for assisting with selecting regions of interest and visualization of results.

W.J.J. consults for Genentech, Biogen, and Bioclinica. All other authors declare no competing financial interests.

Correspondence should be addressed to Jacob Ziontz at jacob_ziontz@berkeley.edu.

<https://doi.org/10.1523/JNEUROSCI.0990-21.2021>

Copyright © 2021 the authors

A developing body of work investigating the mechanisms of tau accumulation supports the transsynaptic propagation of tau via coactive neurons. Studies *in vitro* and in animal models suggest that tau pathology can be transferred between synaptic connections, and that enhanced neuronal activity stimulates the release of pathologic tau and increases downstream accumulation (Pooler et al., 2013; Ahmed et al., 2014; Wu et al., 2016). In humans, transneuronal tau spread has been investigated by associating the topography of tau accumulation with measures of structural and functional connectivity (Cope et al., 2018; Jacobs et al., 2018; Adams et al., 2019; Franzmeier et al., 2019, 2020a,b; Vogel et al., 2020). Connectivity measures between brain regions that exhibit early tau accumulation may therefore provide insights into the structures and processes involved in the spread of tau in aging and AD.

Tau appears to initially propagate to neocortex via connectivity with the anterolateral EC (alEC; Adams et al., 2019), but regions without strong structural connectivity to alEC such as the medial parietal lobe (Van Hoesen et al., 1975; Witter et al., 1989) also develop tau pathology as AD progresses (Maass et al., 2017; Harrison et al., 2019a). Connectivity with other MTL structures that subsequently develop tau pathology, including the posteromedial EC (pmEC) and hippocampus (HC), may thus underlie tau spread into medial parietal lobe. This region also comprises a large part of the posterior medial (PM) memory network, which together with the anterior temporal (AT) memory network represent two distinct large-scale neocortical memory systems with separable anatomic and functional connectivity with the MTL that support different aspects of memory and cognitive function (Ranganath and Ritchey, 2012; Ritchey et al., 2015). Given the substantial increase in PM tau in mild cognitive impairment (MCI) and AD (Maass et al., 2019), tau accumulation in regions of this memory system may be a key condition under which memory performance begins to worsen before the clinical presentation of disease.

In this study, we investigate how tau spreads from MTL to the medial parietal lobe using resting state functional magnetic resonance imaging (fMRI) in a sample of cognitively normal older adults. We measured functional connectivity between key MTL subregions (alEC, pmEC, and HC) and medial parietal lobe, and tested whether this connectivity was related to tau deposition in medial parietal lobe. Given strong structural connectivity between HC and medial parietal lobe (Chrastil, 2018), we hypothesized that the degree of functional connectivity with HC would better predict tau burden in medial parietal lobe than functional connectivity with either entorhinal subregion. Because pmEC also demonstrates connectivity with some medial parietal areas (Witter et al., 1989) and alEC is the earliest cortical region of tau accumulation, we also tested whether these structures would contribute to medial parietal tau. Further, we were interested in examining how connectivity between the MTL and medial parietal lobe was related to both the correspondence of tau between the two regions and to memory function. We hypothesized that MTL and medial parietal tau would be more correlated as functional connectivity between these regions increased, and that greater tau burden and functional connectivity together would be associated with worse memory performance.

Materials and Methods

Participants

To test these hypotheses, we included data from 97 male and female cognitively normal older adults from the Berkeley Aging Cohort Study. All participants underwent 3T structural MRI, and resting state 3T fMRI,

Table 1. Participant characteristics

	Mean (SD) or <i>n</i> (%)	Range
Age (years)	76.4 (6.1)	60–93
Education (years)	16.8 (1.9)	12–20
MMSE	28.6 (1.3)	25–30
Global A β PET	1.17 (0.25)	0.92–1.89
Sex (female)	58 (59.8)	
A β +	43 (45.7)	
APOE ϵ 4+	28 (29.8)	

Demographic information for sample of 97 cognitively normal older adults including age, years of education, mini mental state examination (MMSE) score, global A β PET signal, sex, A β positivity status (A β +), and apolipoprotein E positivity status (APOE ϵ 4+).

and a standard neuropsychological assessment. These participants also received tau PET imaging using ¹⁸F-Flortaucipir (FTP) and A β PET imaging using ¹¹C-Pittsburgh Compound B (PiB). Demographic information for all participants is shown in Table 1. There were three individuals who did not have PiB PET data available for analysis, and so were excluded from all analyses that adjusted for global A β signal. We included only participants whose resting state fMRI data were collected within 146 d of their corresponding tau PET scan (mean = 42.5, SD = 37.9). Additional inclusion criteria for this study were 60+ years of age, cognitively normal status (mini mental state examination score \geq 25 and normal neuropsychological examination, defined as within 1.5 SDs of age, education, and sex adjusted norms), no serious neurologic, psychiatric, or medical illness, no major contraindications found on MRI or PET, and independent community living status. This study was approved by the Institutional Review Boards of the University of California, Berkeley, and the Lawrence Berkeley National Laboratory (LBNL). All participants provided written informed consent.

MRI acquisition

Structural MRI and fMRI data were acquired on a 3T TIM/Trio scanner (Siemens Medical System, software version B17A) using a 32-channel head coil. A T1-weighted whole brain magnetization prepared rapid gradient echo (MPRAGE) image was acquired for each subject (voxel size = 1 mm isotropic, TR = 2300 ms, TE = 2.98 ms, matrix = 256 \times 240 \times 160, FOV = 256 \times 240 \times 160 mm³, sagittal plane, 160 slices, 5-min acquisition time). Resting state fMRI was then acquired using T2*-weighted echoplanar imaging (EPI; voxel size = 2.6 mm isotropic, TR = 1.067 ms, TE = 31.2 ms, FA = 45, matrix 80 \times 80, FOV = 210 mm, sagittal plane, 300 volumes, anterior to posterior phase encoding, ascending acquisition, 5-min acquisition time). During resting state acquisition, participants were told to remain awake with eyes open and focused on a white asterisk displayed on a black background.

MRI preprocessing

Structural T1-weighted images were processed using Statistical Parametric Mapping (SPM12). Images were first segmented into gray matter, white matter, and CSF components in native space. DARTEL-imported tissue segments for all individuals in the sample were used to create a study-specific template, which was then used to warp native space T1 images and tissue segments to MNI space at 2-mm isotropic resolution. Finally, native space T1 images were segmented with Freesurfer v.5.3.0 using the Desikan–Killany atlas parcellation (Desikan et al., 2006).

Resting state fMRI images were preprocessed using a standard SPM12 pipeline. Slice time correction was first applied to adjust for differences in acquisition time for each brain volume. Then, all EPIs were realigned to the first acquired EPI, and translation and rotation realignment parameters were output. Each EPI was next coregistered to each individual's native space T1 image. Next, all resting state EPIs and structural images were warped to the study-specific DARTEL template in 2-mm isotropic MNI space from structural preprocessing. Unsmoothed

fMRI data in MNI space was used to extract the time series correlation of all region of interest (ROI) seeds used in these analyses.

ROIs

We defined ROIs for these analyses to examine the association of functional connectivity between these areas and tau burden. Most were obtained from the FreeSurfer segmentation of each participant's native space 3T structural image (Desikan et al., 2006), including HC, retrosplenial cortex (RsC), posterior cingulate cortex (PCC), precuneus cortex (PrC), whole EC, and inferior temporal cortex (IT). In the case of RsC, we used the FreeSurfer region analog labeled as "isthmus cingulate." The composite medial parietal lobe ROI used throughout this study consisted of the RsC, PCC, and PrC regions. To test neocortical connectivity with HC outside of the medial parietal lobe, we also identified a region in the superior frontal gyrus (SFG) analogous to the medial portion of Brodman area 10, labeled as A10m in the Brainnetome atlas parcellation (Fan et al., 2016).

aEC and pmEC were defined in a previous study with high-resolution 7T MRI (Maass et al., 2015). In brief, anatomic borders of the entire EC were manually defined on a high-resolution T1-group template. Multivariate classification in a group of young adults was used to then identify clusters of voxels within this mask that showed preferential functional connectivity with perirhinal cortex, comprising the aEC ROI, or with the parahippocampal gyrus, comprising the pmEC ROI. These aEC and pmEC ROIs were then warped to a 2-mm isotropic MNI template and made publicly available. In this study, we used these bilateral MNI space ROIs in our functional connectivity analyses. Because these regions are in close spatial proximity to one another, we extracted time series from the unsmoothed, denoised MNI space resting state data to avoid smoothing signal from each seed into each other.

To address signal dropout in the identified ROIs, we derived an explicit mask to remove regions of low signal across the whole brain. This mask was defined by calculating the mean functional MNI space image across all individuals, restricted to a group level gray matter mask. We then excluded voxels with <40% of the mean signal intensity of the image. Using this mean signal intensity threshold mask, a mean of 15.8% of voxels (SD = 11.9%) were removed across all ROIs with the highest proportion of voxels being removed from the A10m region (34.8%).

Functional connectivity analyses

Seed-to-seed functional connectivity was assessed using the CONN functional connectivity toolbox (version 17e; Whitfield-Gabrieli and Nieto-Castanon, 2012) implemented in MATLAB version 2019b (The MathWorks Inc.). ART motion detection was first performed to identify volumes of high motion, using a movement threshold of >0.5 mm/TR and a global intensity z score of 3. Outlier volumes were flagged and included as spike regressors during denoising. No individuals were excluded from these analyses because of excess motion, as all participants had <20% of outlier volumes (mean = 5.0%, SD = 3.4%). Denoising was then performed with translation and rotation realignment parameters and their first-order derivatives, as well as anatomical CompCor (first five components of time series signal from white matter and CSF). A band pass filter of 0.008–0.1 Hz and linear detrending were then applied to the residual time-series.

We constructed a model of functional connectivity between each of three MTL regions (aEC, pmEC, and HC) and medial parietal lobe using bilateral ROIs. Within the medial parietal lobe, we identified the RsC as a region where tau is thought to spread to the neocortex via the MTL (Braak and Braak, 1995) and with known structural and functional connectivity with MTL (Witter et al., 1989; Ranganath and Ritchey, 2012; Chrastil, 2018). Semipartial correlations and unsmoothed data were used to minimize spillover of signal between adjacent MTL regions. Connectivity strength was defined as β -weights from region-to-region semipartial correlations adjusted for age and sex.

PET acquisition and processing

PET was acquired for all participants at LBNL. Tau accumulation was assessed with FTP synthesized at the Biomedical Isotope Facility at

LBNL as previously described (Schöll et al., 2016). Data were collected on a Biograph TruePoint 6 scanner (Siemens, Inc) 75–115 min after injection in listmode. Data were then binned into 4×5 min frames from 80–100 min after injection. CT scans were performed before the start of each emission acquisition. $A\beta$ burden was assessed using PiB, also synthesized at the Biomedical Isotope Facility at LBNL (Mathis et al., 2009). Data were collected on the Biograph scanner across 35 dynamic frames for 90 min after injection and subsequently binned into 35 frames (4×15 , 8×30 , 9×60 , 2×180 , 10×300 , and 2×600 s), and a computed tomography (CT) scan was performed. All PET images were reconstructed using an ordered subset expectation maximization algorithm, with attenuation correction, scatter correction, and smoothing with a 4-mm Gaussian kernel.

Processing of FTP images was conducted in SPM12. Images were realigned, averaged, and coregistered to 3T structural MRIs. Standardized uptake value ratio (SUVR) images were calculated by averaging mean tracer uptake over the 80- to 100-min data and normalized with an inferior cerebellar gray reference region (Baker et al., 2017). The mean SUVR of each ROI (structural MRI FreeSurfer segmentation) was extracted from the native space images. This ROI data were partial volume corrected using a modified Geometric Transfer Matrix approach (Rousset et al., 1998) as previously described (Baker et al., 2017). SUVR images were then warped to 2-mm MNI space for voxelwise analyses using the study-specific DARTEL template produced from structural data (see above). No additional spatial smoothing was applied. PiB images were also realigned using SPM12. An average of frames within the first 20 min was used to calculate the transformation matrix to coregister the PiB images to the participants' 3T structural MRI; this transformation matrix was then applied to all PiB frames. Distribution volume ratio (DVR) images were calculated with Logan graphical analysis over 35–90 min data and normalized to a whole cerebellar gray reference region (Logan, 2000; Price et al., 2005). Global $A\beta$ was calculated across cortical FreeSurfer ROIs as previously described (Mormino et al., 2012), and a threshold of $DVR > 1.065$ was used to categorize participants as $A\beta$ -positive or $A\beta$ -negative. In addition, mean DVR within each FreeSurfer ROI was extracted from coregistered, MNI space PiB images.

Tau PET quantification

To quantify tau deposition, we used the proportion of voxels above an a priori threshold of $SUVR > 1.4$ for FTP PET signal. This threshold has been shown to be a reliable marker of AD-related tau pathology, outperforming other thresholds in discriminating between $A\beta$ -negative older adults and MCI/AD individuals (Maass et al., 2017). This suprathreshold measure has also been used in previous investigation of the relationship between functional connectivity and tau accumulation (Adams et al., 2019). Another distinct advantage of using suprathreshold signal over mean SUVR is that it is not confounded by differing number of voxels within ROIs. To calculate this suprathreshold tau measure for each individual, we computed the number of suprathreshold FTP voxels within each ROI and divided by the total number of voxels in the region. In MTL and particularly HC, however, measuring tau is challenging given the confound of signal contamination from off-target FTP binding in choroid plexus. To address this, we quantified hippocampal tau using Rousset geometric transfer matrix partial volume corrected FTP SUVR, which minimizes choroid plexus spillover (Baker et al., 2017). As an additional precaution, we adjusted for choroid plexus FTP signal in regression analyses using this hippocampal tau signal.

Neuropsychological assessment

To assess episodic memory in our sample of cognitively normal older adults, we used neuropsychological assessment data collected closest in time to each individual's tau scan. There was a mean of 84.2 d (SD = 56.9) between each individual's cognitive assessment and tau PET scan. We computed an episodic memory composite measure by averaging the z -transformed individual test scores using mean and SD from the sample (Maass et al., 2018; Harrison et al., 2019b) for four different

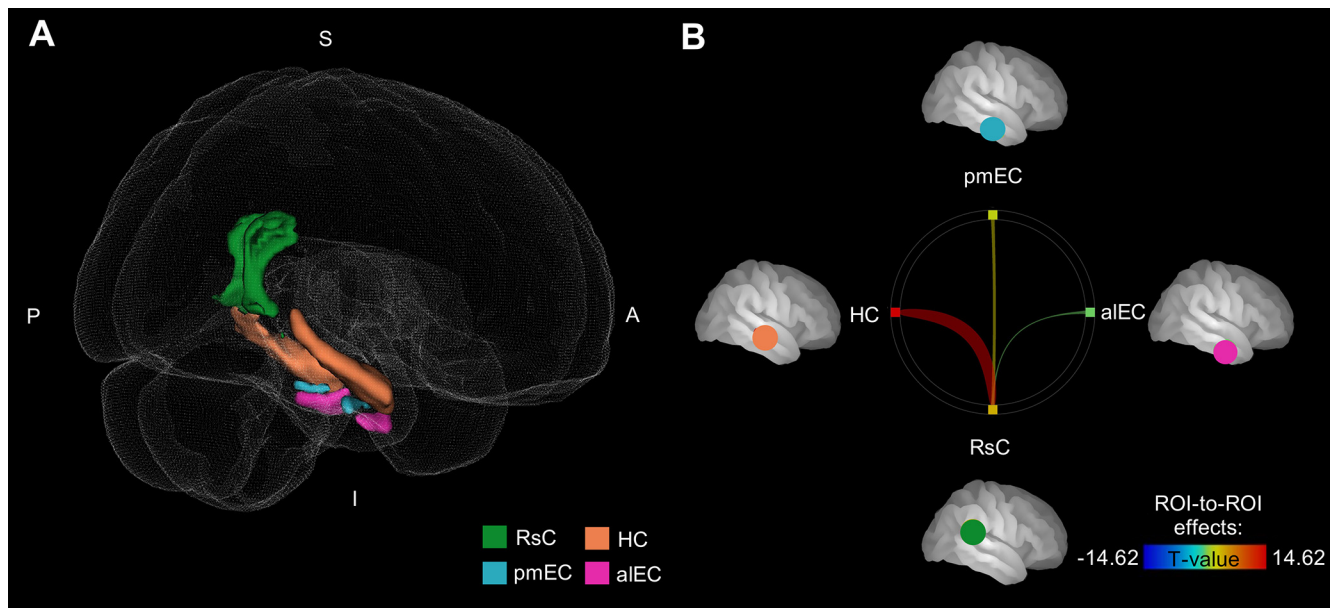


Figure 1. HC exhibits strong resting state functional connectivity with RsC. **A**, ROIs for functional connectivity analysis. aIEC, pmEC, and HC were included from MTL, as well as RsC. **B**, RsC exhibits functional connectivity with HC and pmEC but not aIEC. Line color and thickness correspond to t statistic of one-sample t test of β values. See Extended Data Figure 1-1 for resting state connectivity with SFG and association with medial parietal tau.

tasks. These tasks were the California Verbal Learning Test (CVLT) immediate free recall, CVLT long-delay free recall, Visual Reproduction I (immediate recall), and Visual Reproduction II (delayed recall). We analyzed distinct verbal and visuospatial episodic memory components by considering performance in CVLT and Visual Reproduction tasks separately.

Experimental design and statistical analyses

Functional connectivity analyses were conducted in the CONN functional connectivity toolbox (version 17e). Semipartial correlations were used for all first-level analyses to compute the time series correlation for all voxels of each ROI, controlling for the variance of all other ROIs entered into the same model. Statistically significant functional connectivity was determined by extracting β -weights from region-to-region semipartial correlations adjusted for age and sex. A one-sample t test was then conducted on these β values to test whether connectivity between ROI pairs was significantly different from 0 (two-tailed, false discovery rate corrected $p < 0.05$). Multivariate linear regression analyses were conducted in R (version 3.6.3) with a two-tailed significance level of $\alpha = 0.05$ throughout. All regression analyses were adjusted for age at time of tau scan, sex, and mean global $A\beta$ burden. Analyses involving cognitive test performance were additionally adjusted for years of education and practice effects, quantified as the square root of the number of prior testing occasions (Vonk et al., 2020). All models including interactions used mean-centered values for independent variables.

Results

HC exhibits strong resting state functional connectivity with RsC

We first investigated which structures of the MTL exhibit resting state functional connectivity with RsC, focusing on three ROIs within MTL: aIEC, pmEC, and HC (Fig. 1A). We observed significant functional connectivity between HC and RsC ($\beta = 0.45$, $p < 0.001$), as well as between pmEC and RsC ($\beta = 0.07$, $p = 0.007$). We directly compared the connectivity of these two pathways and found that hippocampal-retrosplenial (HC-RsC) connectivity was significantly greater than pmEC-RsC connectivity (two-tailed paired samples $t_{(96)} = 15.74$, $p < 0.001$). By contrast, no significant connectivity was observed between aIEC and

RsC ($\beta = 0.00$, $p = 0.891$). Thus, HC and to a lesser extent pmEC, but not aIEC, exhibited resting state functional connectivity with RsC in our sample of cognitively normal older adults (Fig. 1B).

HC-RsC connectivity strength is related to medial parietal tau pathology

Having observed strong functional connectivity between MTL and RsC, we next sought to investigate the extent to which this connectivity is associated with tau pathology in a medial parietal lobe composite region comprising the RsC, PrC, and PCC. To visualize this tau signal, we computed the proportion of participants above threshold in each voxel of the composite region. (Fig. 2A). Adjusting for age, sex, and global $A\beta$ PET signal, we found that HC-RsC connectivity strength was associated with suprathreshold tau in the medial parietal lobe ($\beta = 0.145$, $p = 0.004$; Fig. 2B). From this same model, global $A\beta$ was also associated with suprathreshold medial parietal tau ($\beta = 0.113$, $p = 0.014$). In contrast with HC-RsC connectivity, neither aIEC-RsC ($\beta = 0.120$, $p = 0.145$) nor pmEC-RsC connectivity strength ($\beta = 0.015$, $p = 0.842$) were associated with medial parietal lobe tau (Fig. 2C,D) adjusting for age, sex, and global $A\beta$. In a separate model, we further examined whether individuals with more global $A\beta$ exhibited a stronger relationship between HC-RsC and medial parietal tau. Adjusting for age and sex, we did not observe a significant interaction between HC-RsC connectivity and global $A\beta$ ($\beta = 0.442$, $p = 0.141$).

To confirm that the relationship between HC-RsC connectivity and medial parietal tau was specific to RsC and not a general effect of strong resting state functional connectivity, we identified a control region within the SFG analogous to the medial portion of Brodmann area 10 from the Brainnetome Atlas (Fan et al., 2016). Like RsC, this region is known to be part of the default mode network but does not have extensive structural connections with HC and exhibited low signal dropout in our sample. Similar to RsC, we observed significant resting state functional connectivity between HC and SFG ($\beta = 0.40$, $p < 0.001$),

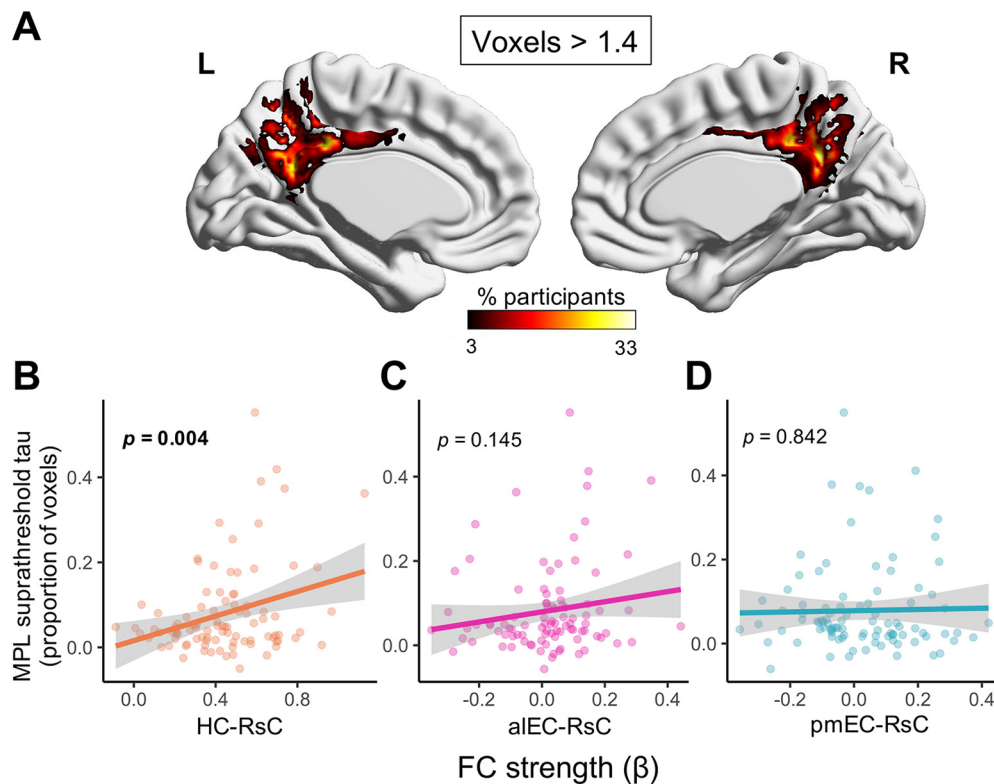


Figure 2. HC-RsC connectivity strength is related to medial parietal tau pathology. **A**, Percent of participants above tau threshold (FTP SUVR > 1.4) for each voxel in medial parietal lobe (MPL) region comprising RsC, PrC, and PCC. **B**, Adjusting for age, sex, and global $A\beta$, HC-RsC resting state functional connectivity strength is associated with mean suprathreshold tau within MPL. MPL suprathreshold tau defined as proportion of voxels above threshold within composite region. aIEC-RsC (**C**) and pmEC-RsC (**D**) connectivity strength are not associated with MPL tau. Significance value for each plot corresponds to effect of each term from linear regression model. Functional connectivity (FC) strength quantified as β values from semipartial correlations between regions. Error bars indicate 95% confidence interval. See Extended Data Figure 2-1 for association between HC-RsC connectivity and tau outside of medial parietal lobe, as well as medial parietal $A\beta$.

although not between SFG and aIEC ($\beta = 0.02$, $p = 0.439$) or pmEC ($\beta = -0.02$, $p = 0.379$; Extended Data Fig. 1-1A). However, in contrast with RsC, we did not observe an association between the strength of HC-SFG connectivity and medial parietal lobe tau ($\beta = 0.006$, $p = 0.907$; Extended Data Fig. 1-1B).

We further wanted to verify that connectivity between HC and RsC was associated specifically with tau in medial parietal lobe and not also in other early tau-accumulating regions. To this end, we examined tau within EC and IT, a region frequently used as a marker for early tau accumulation in aging (Schultz et al., 2017; Huijbers et al., 2019). Again adjusting for age, sex, and global $A\beta$, we found that HC-RsC connectivity was not associated with suprathreshold tau in the EC ($\beta = -0.017$, $p = 0.843$; Extended Data Fig. 2-1A). Although suprathreshold tau in medial parietal lobe and IT were highly correlated (Pearson's $r = 0.796$, $p < 0.001$), HC-RsC was only associated at trend level with inferior temporal tau ($\beta = 0.150$, $p = 0.082$; Extended Data Fig. 2-1B). Finally, to confirm that the relationship between connectivity and pathology was specific to tau, we examined the association between HC-RsC burden in the medial parietal lobe. Adjusting for age and sex, HC-RsC connectivity was not associated with medial parietal lobe $A\beta$ PET signal ($\beta = 0.172$, $p = 0.193$; Extended Data Fig. 2-1C). Taken together, these results demonstrate the specificity of tau pathology accumulation in medial parietal lobe via direct connectivity with HC in cognitively unimpaired older adults.

HC-RsC connectivity strengthens tau correspondence

To further examine the role of functional connectivity in the accumulation of tau pathology from MTL, we tested whether

Table 2. Summary of model results with medial parietal tau as outcome

Independent variables:	Dependent variable: MPL suprathreshold tau
Age	$\beta = -0.002$ $p = 0.321$
Sex	$\beta = 0.007$ $p = 0.708$
Global $A\beta$	$\beta = 0.050$ $p = 0.241$
Choroid plexus signal	$\beta = -0.012$ $p = 0.208$
HC mean tau	$\beta = 0.263^{***}$ $p < 0.001$
HC-RsC FC strength	$\beta = 0.123^{**}$ $p = 0.005$
HC mean tau \times HC-RsC FC strength	$\beta = 0.607^{**}$ $p = 0.008$
Constant	$\beta = 0.066$ $p = 0.281$

Effects from linear regression model examining the relationship between medial parietal lobe (MPL) suprathreshold tau and age, sex, global $A\beta$, choroid plexus signal (partial volume corrected FTP SUVR), HC mean tau (partial volume corrected FTP SUVR), HC-RsC functional connectivity (FC) strength, and HC mean tau \times HC-RsC FC strength interaction. Bolded term indicates interaction effect visualized in Figure 3. See Extended Data Table 2-1 for model results using FTP SUVR from EC instead of HC; * $p < 0.05$, ** $p < 0.01$, *** $p < 0.001$.

HC-RsC connectivity strength modulated how closely MTL tau corresponded with medial parietal lobe tau. Adjusting for age, sex, global $A\beta$, and choroid plexus FTP signal, there was a significant main effect of hippocampal tau ($\beta = 0.263$, $p < 0.001$) as

well as a main effect of HC-RsC ($\beta = 0.123$, $p = 0.005$) on medial parietal lobe suprathreshold tau (Table 2). Critically, we also observed an interaction between hippocampal tau and HC-RsC connectivity ($\beta = 0.607$, $p = 0.008$; Fig. 3) such that there was a stronger association between MTL and medial parietal lobe tau with greater functional connectivity between these regions. To further verify that choroid plexus spillover into HC was not driving these results, we replicated this analysis using partial volume corrected entorhinal tau PET, and found a trend-level interaction between entorhinal tau and HC-RsC in predicting medial parietal tau ($\beta = 0.357$, $p = 0.073$; Extended Data Fig. 3-1). Because tau in EC and HC were highly correlated with one another (Pearson's $r = 0.719$, $p < 0.001$), it is not surprising that using entorhinal tau yielded a similar result, and suggests that contamination of hippocampal signal from non-specific choroid plexus FTP binding is likely not driving this finding.

Episodic memory is related to an interaction between tau and connectivity

We next sought to test whether connectivity and tau might also interact to associate with episodic memory performance. Adjusting for age, years of education, practice effects, and global $A\beta$, we did not observe a significant main effect of either medial parietal lobe tau ($\beta = 1.111$, $p = 0.318$) or HC-RsC connectivity ($\beta = 0.073$, $p = 0.861$) on episodic memory. Critically, there was a significant interaction between medial parietal tau and HC-RsC connectivity ($\beta = -9.482$, $p = 0.018$), such that episodic memory performance was poorest when both medial parietal tau and HC-RsC connectivity were greatest (Table 3). Examining episodic memory subdomains separately, the interaction between medial parietal tau and HC-RsC connectivity was significantly associated with visuospatial memory performance ($\beta = -12.016$, $p = 0.006$; Fig. 4A), but not verbal memory performance ($\beta = -6.933$, $p = 0.145$; Fig. 4B).

Discussion

In this study of cognitively unimpaired older adults, we measured functional connectivity between the MTL and medial parietal lobe using resting state fMRI and examined tau and $A\beta$ pathology with PET imaging. Overall, our findings suggest that AD-related tau accumulates in medial parietal lobe via connectivity with HC, and that this may reflect early disruption of memory processing via tau spread. A growing literature has linked patterns of resting state functional connectivity to greater tau accumulation and correspondence of tau between these regions (Adams et al., 2019; Franzmeier et al., 2019). Although recent data suggest heterogeneity in patterns of tau deposition in patients with AD, these distinct profiles all include medial parietal lobe as a vulnerable region (Vogel et al., 2021). Further, computational modeling of tau spread using functional connectivity closely resembles the observed pattern of tau deposition in the brain (Cope et al., 2018; Vogel et al., 2020). Our finding that connectivity between RsC and HC, but not aIEC or pmEC, was associated with medial parietal tau suggests that tau originating in

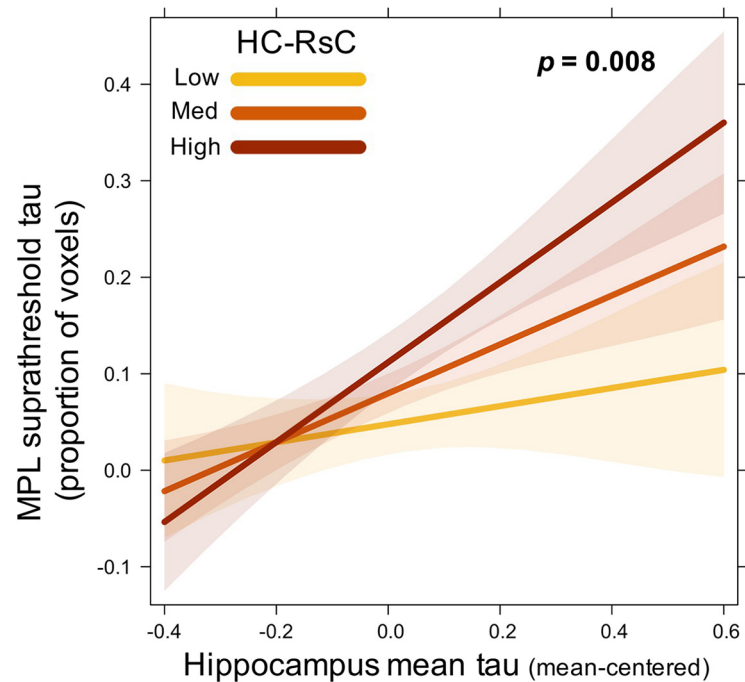


Figure 3. HC-RsC connectivity modulates the relationship between medial temporal and medial parietal tau. Visualization of interaction between HC mean tau (partial volume corrected FTP SUVR) and HC-RsC functional connectivity strength (HC-RsC) from linear regression model (see Table 2). Medial parietal lobe (MPL) suprathreshold tau is associated with a hippocampal tau \times HC-RsC interaction. Plot displays the relationship predicted by linear regression at low (10th percentile), median, and high (90th percentile) HC-RsC. Error bars indicate 95% confidence interval. See Extended Data Figure 3-1 for visualization of the same interaction effect using FTP SUVR from EC in place of HC.

Table 3. Summary of model results with episodic memory performance as outcome

Independent variables:	Dependent variable: Episodic memory composite
Age	$\beta = -0.048^{**}$ $p = 0.005$
Sex	$\beta = -0.105$ $p = 0.540$
Years of education	$\beta = 0.037$ $p = 0.420$
Practice effects	$\beta = 0.253^{*}$ $p = 0.019$
Global $A\beta$	$\beta = -0.308$ $p = 0.395$
MPL suprathreshold tau	$\beta = 1.130$ $p = 0.284$
HC-RsC FC strength	$\beta = 0.079$ $p = 0.843$
MPL suprathreshold tau \times HC-RsC FC strength	$\beta = -9.531^{*}$ $p = 0.018$
Constant	$\beta = 0.139$ $p = 0.772$

Effects from linear regression model examining the relationship between episodic memory performance (CVLT immediate and long-delay free recall, Visual Reproduction immediate and delay recall) and age, years of education, practice effects (see Materials and Methods), global $A\beta$, MPL suprathreshold tau, HC-RsC FC strength, and MPL suprathreshold tau \times HC-RsC FC strength interaction. Bolded term indicates interaction effect visualized in Figure 4; $*p < 0.05$, $**p < 0.01$, $***p < 0.001$.

MTL accumulates in HC before later spreading directly to medial parietal lobe via connectivity with RsC. Because pmEC-RsC connectivity was weaker than HC-RsC connectivity and did not correlate with medial parietal tau, it is not likely to be the primary structure involved in the propagation of tau to this region despite

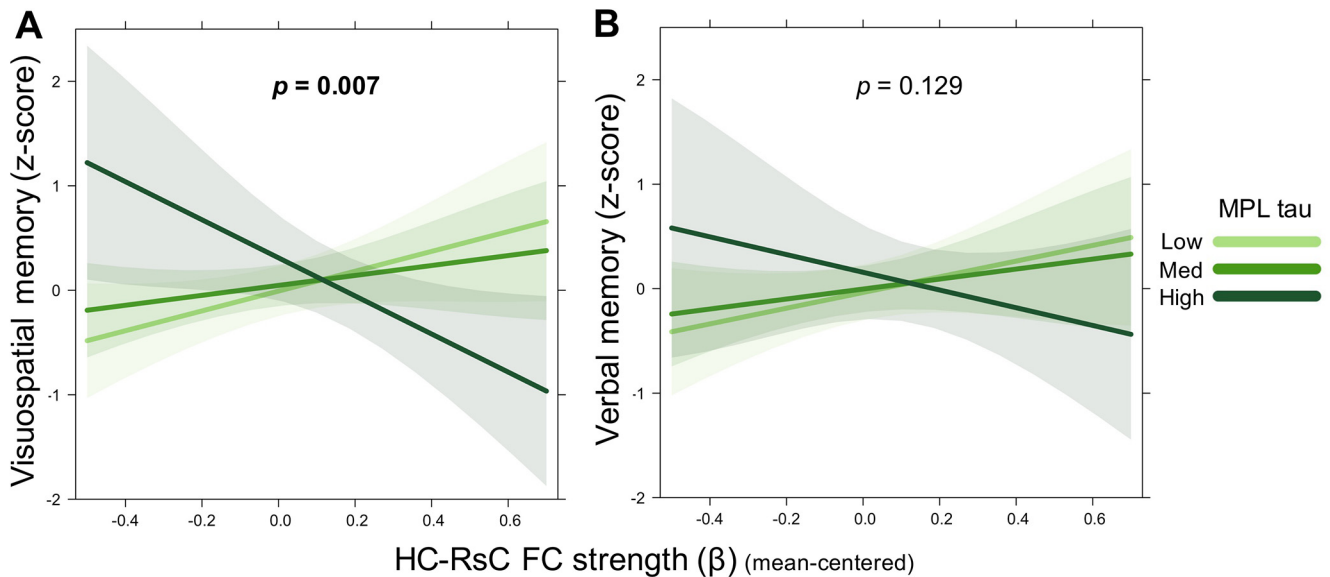


Figure 4. Episodic memory performance is associated with the interaction of HC-RsC connectivity and medial parietal tau. Visualization of interaction between HC-RsC functional connectivity (FC) strength (β value) and medial parietal lobe (MPL) suprathereshold tau in relation to visuospatial and verbal memory, adjusting for age, sex, years of education, practice effects, and global $A\beta$. **A**, Visuospatial memory (Visual Reproduction immediate and delay recall) is associated with the interaction of MPL tau and HC-RsC FC strength. **B**, Verbal memory (CVLT immediate and long delay free recall) does not exhibit a significant interaction. Plots display the relationship predicted by linear regression at low (10th percentile), median, and high (90th percentile) MPL suprathereshold tau. Error bars indicate 95% confidence interval.

connectivity with several posterior medial areas (Navarro Schröder et al., 2015; Adams et al., 2019).

Instead, tau may spread to aEC-connected neocortex and HC at a comparable rate, later accumulating in medial parietal areas with connections to the HC. This is consistent with histopathological data indicating that although the earliest cortical region to exhibit tau pathology is the aEC/transentorhinal area (Braak and Braak, 1985; Kaufman et al., 2018), tau is typically observed in HC before limbic areas such as the retrosplenial region (Braak and Braak, 1995). Our findings also corroborate recent work that found that structural connectivity between HC and PCC was associated with tau pathology in PCC (Jacobs et al., 2018). Importantly, our finding of greater correspondence between hippocampal and medial parietal tau with greater HC-RsC connectivity strength further suggests that neural connectivity may reflect patterns of tau spread from early-accumulating regions to connected downstream areas.

The specificity of this key finding in our study is striking. The lack of association between HC-RsC connectivity and tau in EC suggests this connectivity is specifically related to tau in the downstream medial parietal region of this pathway. Although the IT is one of the first areas of neocortical tau pathology and is often used as a marker of AD disease progression (Schultz et al., 2017; Huijbers et al., 2019), we found the strength of HC-RsC connectivity was only associated at trend level with tau in this region. In addition, functional connectivity between HC and the SFG was significant but not associated with medial parietal tau, suggesting that functional connections with other brain areas are not related to tau in medial parietal lobe. We also did not find an association between HC-RsC and $A\beta$ burden within medial parietal lobe, which is not surprising given that $A\beta$ does not originate in the MTL and is not thought to spread in the same transneuronal manner as tau. Taken together, these results support the view that tau pathology in HC spreads to medial parietal lobe in cognitively unimpaired older adults, reflected by resting state functional connectivity between these regions.

Some studies have in fact found a negative association between tau pathology and functional connectivity across the cortex (Schultz et al., 2017; Sepulcre et al., 2017; Berron et al., 2020), although these tended to use global measures of tau or focused on $A\beta$ -positive individuals. However, our findings together with previous work help illustrate how the relationship between tau and connectivity may vary between different brain areas and time scales. Initially, greater connectivity within an individual pathway may facilitate the spread of tau from regions of early accumulation to downstream cortical areas, perhaps enhanced by the presence of $A\beta$. Over time, however, the influence of tau throughout this circuit leads to neurodegeneration and disruption of neuronal signaling, and tau pathology may in fact show an inverse correlation with functional connectivity. These distinct short-term and long-term effects may help explain regional differences in the tau-connectivity relationship such that pathways of early tau propagation are first to show local degeneration, whereas later pathways, such as the MTL-medial parietal lobe, may concurrently demonstrate increased connectivity leading to further tau spread.

We also found that episodic memory performance, particularly visuospatial memory, was related to the combination of greater medial parietal lobe tau accumulation and greater HC-RsC strength. Because we did not observe a main effect of connectivity on memory, it does not appear likely that greater connectivity alone is related to worse cognition. However, the interaction between connectivity strength and medial parietal tau suggests that the presence of tau in conjunction with greater connectivity along this pathway may indeed be detrimental for memory performance. Existing work has yet to establish a clear relationship between memory performance and connectivity changes in aging. Greater functional connectivity between MTL and medial parietal areas is related to poorer memory performance both cross-sectionally and over time (Berron et al., 2020). By contrast, a positive association has been reported between MTL-medial parietal connectivity and memory performance (Wang et al., 2010; Kaboodvand et al., 2018), although these studies did not include tau PET measures. Abnormal diffusivity

of the hippocampal cingulum bundle has also been shown to be related to greater decline in memory performance in older individuals with high PCC tau and high $A\beta$ (Jacobs et al., 2018).

It may be that the propagation of tau, reflected by greater connectivity and correspondence of pathology between regions, is associated with the earliest deficits in cognitive function. Converging theoretical frameworks including the “molecular nexopathies” paradigm have proposed that the conjunction of pathology and intrinsic circuit characteristics can lead to a state of mild peptide-dependent network disruption, marking the onset of neurodegenerative disease (Warren et al., 2013; Harris et al., 2020) before widespread neurodegeneration and cascading network failure (Jones et al., 2017). Tau spread to the medial parietal lobe may be an indicator of consequences for the PM memory system, which while not affected by tau as early as the AT system may begin to be disrupted in MCI and AD (Maass et al., 2019). It is also striking that we found a particularly strong association with visuospatial memory, given medial parietal areas have long been implicated in processing of spatial information (Flicker et al., 1984; Bushara et al., 1999; Iachini et al., 2009). The representation of visuospatial context is also thought to be a key function of the PM memory system (Ranganath and Ritchey, 2012), and spatial information processing is one of the earliest-affected domains in cognitive aging and AD (Lithfous et al., 2013). Connectivity-mediated accumulation of tau may thus underlie the beginnings of cognitive decline in healthy older adults.

There are a number of limitations to the conclusions drawn from this study. The cross-sectional and correlational nature of these results means that caution is required in inferring a causal relationship between connectivity and tau spread. Still, in view of longitudinal studies showing that tau propagates to different regions over time via connectivity (Franzmeier et al., 2020a,b), our findings are consistent with a relationship that could be causal. In addition, although we adjusted for $A\beta$ PET signal throughout this study, we did not find that the relationships described here were stronger in individuals with greater global $A\beta$ burden. This was a somewhat surprising finding given a number of studies that have found a stronger association between tau and connectivity for those with greater $A\beta$ pathology (Jacobs et al., 2018; Adams et al., 2019; Franzmeier et al., 2020b). It is possible that our sample did not provide us with enough statistical power to observe this interaction, although it was enriched to include nearly half $A\beta$ -positive individuals. Further study is needed to assess the role of $A\beta$ in the association between medial parietal lobe tau and functional connectivity in cognitively normal older adults.

In conclusion, the findings described here support the view that tau pathology accumulates in medial parietal lobe via direct connectivity with HC in cognitively normal older individuals. Although the accumulation of tau pathology in MTL and even some areas of the AT network has been observed in older adults without cognitive impairment, tau spread into the PM network and subsequent domain-specific memory decline may reflect a significant transition between normal aging and the processes involved in AD. Future work with longitudinal data can help establish tau propagation into the medial parietal lobe as a crucial marker of the beginnings of AD.

References

- Adams JN, Maass A, Harrison TM, Baker SL, Jagust WJ (2019) Cortical tau deposition follows patterns of entorhinal functional connectivity in aging. *Elife* 8:e49132.
- Ahmed Z, Cooper J, Murray TK, Garn K, McNaughton E, Clarke H, Parhizkar S, Ward MA, Cavallini A, Jackson S, Bose S, Clavaguera F, Tolnay M, Lavenir I, Goedert M, Hutton ML, O'Neill MJ (2014) A novel in vivo model of tau propagation with rapid and progressive neurofibrillary tangle pathology: the pattern of spread is determined by connectivity, not proximity. *Acta Neuropathol* 127:667–683.
- Baker SL, Maass A, Jagust WJ (2017) Considerations and code for partial volume correcting [^{18}F]-AV-1451 tau PET data. *Data Brief* 15:648–657.
- Berron D, van Westen D, Ossenkoppele R, Strandberg O, Hansson O (2020) Medial temporal lobe connectivity and its associations with cognition in early Alzheimer's disease. *Brain* 143:1233–1248.
- Braak H, Braak E (1985) On areas of transition between entorhinal allocortex and temporal isocortex in the human brain. Normal morphology and lamina-specific pathology in Alzheimer's disease. *Acta Neuropathol* 68:325–332.
- Braak H, Braak E (1991) Neuropathological staging of Alzheimer-related changes. *Acta Neuropathol* 82:239–259.
- Braak H, Braak E (1995) Staging of Alzheimer's disease-related neurofibrillary changes. *Neurobiol Aging* 16:271–278.
- Bushara KO, Weeks RA, Ishii K, Catalan MJ, Tian B, Rauschecker JP, Hallett M (1999) Modality-specific frontal and parietal areas for auditory and visual spatial localization in humans. *Nat Neurosci* 2:759–766.
- Chrastil ER (2018) Heterogeneity in human retrosplenial cortex: a review of function and connectivity. *Behav Neurosci* 132:317–338.
- Cope TE, Rittman T, Borchert RJ, Jones PS, Vatanserver D, Allinson K, Passamonti L, Vazquez Rodriguez P, Bevan-Jones WR, O'Brien JT, Rowe JB (2018) Tau burden and the functional connectome in Alzheimer's disease and progressive supranuclear palsy. *Brain* 141:550–567.
- Desikan RS, Ségonne F, Fischl B, Quinn BT, Dickerson BC, Blacker D, Buckner RL, Dale AM, Maguire RP, Hyman BT, Albert MS, Killiany RJ (2006) An automated labeling system for subdividing the human cerebral cortex on MRI scans into gyral based regions of interest. *Neuroimage* 31:968–980.
- Fan L, Li H, Zhuo J, Zhang Y, Wang J, Chen L, Yang Z, Chu C, Xie S, Laird AR, Fox PT, Eickhoff SB, Yu C, Jiang T (2016) The human brainnetome atlas: a new brain atlas based on connective architecture. *Cereb Cortex* 26:3508–3526.
- Flicker C, Bartus RT, Crook TH, Ferris SH (1984) Effects of aging and dementia upon recent visuospatial memory. *Neurobiol Aging* 5:275–283.
- Franzmeier N, Rubinski A, Neitzel J, Kim Y, Damm A, Na DL, Kim HJ, Lyoo CH, Cho H, Finsterwalder S, Duering M, Seo SW, Ewers M; Alzheimer's Disease Neuroimaging Initiative (2019) Functional connectivity associated with tau levels in ageing, Alzheimer's, and small vessel disease. *Brain* 142:1093–1107.
- Franzmeier N, Dewenter A, Frontzkowski L, Dichgans M, Rubinski A, Neitzel J, Smith R, Strandberg O, Ossenkoppele R, Buerger K, Duering M, Hansson O, Ewers M (2020a) Patient-centered connectivity-based prediction of tau pathology spread in Alzheimer's disease. *Sci Adv* 6:eabd1327.
- Franzmeier N, Neitzel J, Rubinski A, Smith R, Strandberg O, Ossenkoppele R, Hansson O, Ewers M; Alzheimer's Disease Neuroimaging Initiative (ADNI) (2020b) Functional brain architecture is associated with the rate of tau accumulation in Alzheimer's disease. *Nat Commun* 11:347.
- Harris SS, Wolf F, De Strooper B, Busche MA (2020) Tipping the scales: peptide-dependent dysregulation of neural circuit dynamics in Alzheimer's disease. *Neuron* 107:417–419.
- Harrison TM, La Joie R, Maass A, Baker SL, Swinnerton K, Fenton L, Mellinger TJ, Edwards L, Pham J, Miller BL, Rabinovici GD, Jagust WJ (2019a) Longitudinal tau accumulation and atrophy in aging and Alzheimer disease. *Ann Neurol* 85:229–240.
- Harrison TM, Maass A, Adams JN, Du R, Baker SL, Jagust WJ (2019b) Tau deposition is associated with functional isolation of the hippocampus in aging. *Nat Commun* 10:4900.
- He Z, Guo JL, McBride JD, Narasimhan S, Kim H, Changolkar L, Zhang B, Gathagan RJ, Yue C, Dengler C, Stieber A, Nitla M, Coulter DA, Abel T, Brunden KR, Trojanowski JQ, Lee VMY (2018) Amyloid- β plaques enhance Alzheimer's brain tau-seeded pathologies by facilitating neuritic plaque tau aggregation. *Nat Med* 24:29–38.
- Huijbers W, Schultz AP, Papp KV, LaPoint MR, Hanseuw B, Chhatwal JP, Hedden T, Johnson KA, Sperling RA (2019) Tau accumulation in clinically normal older adults is associated with hippocampal hyperactivity. *J Neurosci* 39:548–556.
- Iachini T, Iavarone A, Senese V, Ruotolo F, Ruggiero G (2009) Visuospatial memory in healthy elderly, AD and MCI: a review. *Curr Aging Sci* 2:43–59.

- Jacobs HIL, Hedden T, Schultz AP, Sepulcre J, Perea RD, Amariglio RE, Papp KV, Rentz DM, Sperling RA, Johnson KA (2018) Structural tract alterations predict downstream tau accumulation in amyloid-positive older individuals. *Nat Neurosci* 21:424–431.
- Johnson KA, Schultz A, Betensky RA, Becker JA, Sepulcre J, Rentz D, Mormino E, Chhatwal J, Amariglio R, Papp K, Marshall G, Albers M, Mauro S, Pepin L, Alverio J, Judge K, Philiosaint M, Shoup T, Yokell D, Dickerson B, et al. (2016) Tau positron emission tomographic imaging in aging and early Alzheimer disease. *Ann Neurol* 79:110–119.
- Jones DT, Graff-Radford J, Lowe VJ, Wiste HJ, Gunter JL, Senjem ML, Botha H, Kantarci K, Boeve BF, Knopman DS, Petersen RC, Jack CR (2017) Tau, amyloid, and cascading network failure across the Alzheimer's disease spectrum. *Cortex* 97:143–159.
- Kaboodvand N, Bäckman L, Nyberg L, Salami A (2018) The retrosplenial cortex: a memory gateway between the cortical default mode network and the medial temporal lobe. *Hum Brain Mapp* 39:2020–2034.
- Kaufman SK, Del Tredici K, Thomas TL, Braak H, Diamond MI (2018) Tau seeding activity begins in the transentorhinal/entorhinal regions and anticipates phospho-tau pathology in Alzheimer's disease and PART. *Acta Neuropathol* 136:57–67.
- Lithfous S, Dufour A, Després O (2013) Spatial navigation in normal aging and the prodromal stage of Alzheimer's disease: insights from imaging and behavioral studies. *Ageing Res Rev* 12:201–213.
- Logan J (2000) Graphical analysis of PET data applied to reversible and irreversible tracers. *Nucl Med Biol* 27:661–670.
- Maass A, Berron D, Libby LA, Ranganath C, Düzel E (2015) Functional sub-regions of the human entorhinal cortex. *Elife* 4:e06426.
- Maass A, Landau S, Horng A, Lockhart SN, Rabinovici GD, Jagust WJ, Baker SL, La Joie R; Alzheimer's Disease Neuroimaging Initiative (2017) Comparison of multiple tau-PET measures as biomarkers in aging and Alzheimer's disease. *Neuroimage* 157:448–463.
- Maass A, Lockhart SN, Harrison TM, Bell RK, Mellinger T, Swinnerton K, Baker SL, Rabinovici GD, Jagust WJ (2018) Entorhinal tau pathology, episodic memory decline, and neurodegeneration in aging. *J Neurosci* 38:530–543.
- Maass A, Berron D, Harrison TM, Adams JN, La Joie R, Baker S, Mellinger T, Bell RK, Swinnerton K, Inglis B, Rabinovici GD, Düzel E, Jagust WJ (2019) Alzheimer's pathology targets distinct memory networks in the ageing brain. *Brain* 142:2492–2509.
- Mathis CA, Wang Y, Holt DP, Huang G, Debnath ML, Klunk WE (2009) Synthesis and evaluation of ¹¹C-labeled 6-substituted 2-arylbenzothiazoles as amyloid imaging agents. *J Med Chem* :1–15.
- Mormino EC, Brandel MG, Madison CM, Rabinovici GD, Marks S, Baker SL, Jagust WJ (2012) Not quite PIB-positive, not quite PIB-negative: slight PIB elevations in elderly normal control subjects are biologically relevant. *Neuroimage* 59:1152–1160.
- Navarro Schröder T, Haak KV, Zaragoza Jimenez NI, Beckmann CF, Doeller CF (2015) Functional topography of the human entorhinal cortex. *Elife* 4:e06738.
- Pooler AM, Phillips EC, Lau DHW, Noble W, Hanger DP (2013) Physiological release of endogenous tau is stimulated by neuronal activity. *EMBO Rep* 14:389–394.
- Price JC, Klunk WE, Lopresti BJ, Lu X, Hoge JA, Ziolkowski SK, Holt DP, Meltzer CC, DeKosky ST, Mathis CA (2005) Kinetic modeling of amyloid binding in humans using PET imaging and Pittsburgh Compound-B. *J Cereb Blood Flow Metab* 25:1528–1547.
- Ranganath C, Ritchey M (2012) Two cortical systems for memory-guided behaviour. *Nat Rev Neurosci* 13:713–726.
- Ritchey M, Libby LA, Ranganath C (2015) Cortico-hippocampal systems involved in memory and cognition: the PMAT framework, Ed 1. Amsterdam: Elsevier B.V.
- Roussot OG, Ma Y, Evans AC (1998) Correction for partial volume effects in PET: principle and validation. *J Nucl Med* 39:904–911.
- Schöll M, Lockhart SN, Schonhaut DR, O'Neil JP, Janabi M, Ossenkoppele R, Baker SL, Vogel JW, Faria J, Schwimmer HD, Rabinovici GD, Jagust WJ (2016) PET imaging of tau deposition in the aging human brain. *Neuron* 89:971–982.
- Schultz AP, Chhatwal JP, Hedden T, Mormino EC, Hanseeuw BJ, Sepulcre J, Huijbers W, LaPoint M, Buckley RF, Johnson KA, Sperling RA (2017) Phases of hyperconnectivity and hypoconnectivity in the default mode and salience networks track with amyloid and tau in clinically normal individuals. *J Neurosci* 37:4323–4331.
- Sepulcre J, Sabuncu MR, Li Q, El Fakhri G, Sperling R, Johnson KA (2017) Tau and amyloid β proteins distinctively associate to functional network changes in the aging brain. *Alzheimers Dement* 13:1261–1269.
- Van Hoesen GW, Pandya DN, Butters N (1975) Some connections of the entorhinal (area 28) and perirhinal (area 35) cortices of the rhesus monkey. II. Frontal lobe afferents. *Brain Res* 95:25–38.
- Vogel JW, Iturria-Medina Y, Strandberg OT, Smith R, Levitis E, Evans AC, Hansson O; Swedish BioFinder Study (2020) Spread of pathological tau proteins through communicating neurons in human Alzheimer's disease. *Nat Commun* 11:2612.
- Vogel JW, Young AL, Oxtoby NP, Smith R, Ossenkoppele R, Strandberg OT, La Joie R, Aksamit LM, Grothe MJ, Iturria-Medina Y, Pontecorvo MJ, Devous MD, Rabinovici GD, Alexander DC, Lyoo CH, Evans AC, Hansson O; Alzheimer's Disease Neuroimaging Initiative (2021) Four distinct trajectories of tau deposition identified in Alzheimer's disease. *Nat Med* 27:871–881.
- Vonk JMJ, Bouteloup V, Mangin J, Dubois B, Blanc F, Gabelle A, Ceccaldi M, Annweiler C, Krolak-Salmon P, Belin C, Rivasseau-Jonveaux T, Julian A, Sellal F, Magnin E, Chupin M, Habert M, Chêne G, Dufouil C (2020) Semantic loss marks early Alzheimer's disease-related neurodegeneration in older adults without dementia. *Alzheimer's Dement Diagnosis. Assess Dis Monit* 12:1–14.
- Wang L, Laviolette P, O'Keefe K, Putcha D, Bakkour A, Van Dijk KRA, Pihlajamäki M, Dickerson BC, Sperling RA (2010) Intrinsic connectivity between the hippocampus and posteromedial cortex predicts memory performance in cognitively intact older individuals. *Neuroimage* 51:910–917.
- Warren JD, Rohrer JD, Schott JM, Fox NC, Hardy J, Rossor MN (2013) Molecular nexopathies: a new paradigm of neurodegenerative disease. *Trends Neurosci* 36:561–569.
- Whitfield-Gabrieli S, Nieto-Castanon A (2012) Conn: a functional connectivity toolbox for correlated and anticorrelated brain networks. *Brain Connect* 2:125–141.
- Witter MP, Groenewegen HJ, Lopes da Silva FH, Lohman AHM (1989) Functional organization of the extrinsic and intrinsic circuitry of the parahippocampal region. *Prog Neurobiol* 33:161–253.
- Wu JW, Hussaini SA, Bastille IM, Rodriguez GA, Mrejeru A, Rilett K, Sanders DW, Cook C, Fu H, Boonen RACM, Herman M, Nahmani E, Emrani S, Figueroa YH, Diamond MI, Clelland CL, Wray S, Duff KE (2016) Neuronal activity enhances tau propagation and tau pathology in vivo. *Nat Neurosci* 19:1085–1092.